Two-Phase Pressure Test Analysis

Arild Bøe, SPE, Rogaland Research Inst., and **Svein M. Skjaeveland,** SPE, and **Curtis H. Whitson,*** SPE, Rogaland U.

Summary. A theoretical basis is given for well test analysis of solution-gas and gas-condensate reservoirs in the infinite-acting period. The study is limited to radial flow with a fully penetrating well in the center of the drainage area. Porosity and absolute permeability are constant, and gravitational and capillary effects are neglected. The tests are conducted at constant surface rate, and the skin factor is zero. An analytical expression for the pressure/saturation relationship is derived from the time-dependent gas and oil flow equations. This relationship can be used to generate pseudopressure functions that allow test interpretation with liquid analogy. The infinite-acting drawdown case is treated in detail, while the buildup case is briefly discussed. Theoretical developments are exemplified by simulated drawdown and buildup tests in a solution-gas-drive reservoir.

Introduction

Many pressure-transient tests can be interpreted by using solutions of the diffusivity equation that are based on the liquid analogy of reservoir fluids. In the liquid model, the reservoir fluids are represented by a single-phase liquid with small and constant compressibility and constant viscosity. The corresponding diffusivity equation is linear, and solutions for a variety of boundary conditions have been presented in the literature. Single-phase gas tests can be interpreted within the liquid analogy by introducing an integral transform, the pseudopressure function, as suggested by Al-Hussainy *et al.*[1] This pseudopressure function is uniquely dependent on pressure and can therefore be used for both drawdown and buildup analyses.

To a certain extent, multiphase flow effects also can be adapted to the liquid model solutions if total mobility and compressibility are used.[2,3] The interpretation of the test will yield the effective permeability. For solution-gas reservoirs, this method becomes less reliable with increasing gas saturation.[4] A better adaptation to the liquid analogy can be achieved by introducing a pseudopressure function into the multiphase-flow equations, as suggested by Fetkovich,[5] in analogy with the single-phase gas case. This suggestion was pursued by Raghavan,[6] who gave practical methods for calculating the pseudopressure function for oil in solution-gas-drive reservoirs and showed that the standard liquid-analogy semilog plots could be used to calculate the absolute formation permeability from computer-generated test data. To evaluate the oil pseudopressure function, the relation between oil saturation and pressure must be known. Raghavan, however, did not present a theoretically based relation but demonstrated, through examples, that the instantaneous producing GOR could be used for drawdown interpretation. He also suggested that the producing GOR at shut-in could be used for buildup analysis.

The objective of this paper is to present theoretical relationships between pressure and saturation that can be used to evaluate pseudopressure functions in the infinite-acting period. The suggested methods are valid for any multiphase system provided that the fluid flow can be described by diffusivity equations based on "beta" formulation—i.e., FVF's. The examples, obtained from computer-generated test data, are limited to solution-gas-drive reservoirs.

Theory

For simplicity, consider only the oil and gas phases to be mobile and the irreducible water to be incompressible. The flow equations for gas and oil, respectively, are then

$$\nabla\cdot\left[\left(\frac{R_s k_{ro}}{\mu_o B_o}+\frac{k_{rg}}{\mu_g B_g}\right)\nabla p\right]=\frac{\phi}{k}\frac{\partial}{\partial t}\left(\frac{R_s S_o}{B_o}+\frac{S_g}{B_g}\right) \quad \ldots\ldots (1)$$

$$\text{and } \nabla\cdot\left[\left(\frac{r_s k_{rg}}{\mu_g B_g}+\frac{k_{ro}}{\mu_o B_o}\right)\nabla p\right]=\frac{\phi}{k}\frac{\partial}{\partial t}\left(\frac{r_s S_g}{B_g}+\frac{S_o}{B_o}\right), \quad \ldots\ldots (2)$$

where $S_o+S_g+S_{iw}=1$, R_s=gas dissolved in the oil phase, and r_s=oil dissolved in the gas phase. This last term is included to make the system of equations applicable to gas-condensate reservoirs. In this case, the FVF's, B_o, r_s, R_s, and B_g, can be derived from a constant-volume-depletion experiment, as proposed by Whitson and Torp.[7]

The following simplifying notation is introduced.

$$S\equiv S_o, \quad \ldots\ldots (3a)$$

$$a\equiv R_s k_{ro}/\mu_o B_o+k_{rg}/\mu_g B_g, \quad \ldots\ldots (3b)$$

$$\alpha\equiv r_s k_{rg}/\mu_g B_g+k_{ro}/\mu_o B_o, \quad \ldots\ldots (3c)$$

$$b\equiv R_s S_o/B_o+S_g/B_g, \quad \ldots\ldots (3d)$$

$$\text{and } \beta\equiv r_s S_g/B_g+S_o/B_o. \quad \ldots\ldots (3e)$$

In these expressions, R_s, r_s, B_o, B_g, μ_o, and μ_g depend only on p, while k_{rg} and k_{ro} depend only on S. Consistent units are assumed.

We also introduce $\dot{x}\equiv(\partial x/\partial S)_p$ and $x'\equiv(\partial x/\partial p)_S$ for the partial derivative with respect to saturation at constant pressure and the partial derivative with respect to pressure with saturation held constant, where $x\in(a, \alpha, b, \beta)$. Eqs. 1 and 2 may then be written as

$$\nabla\cdot(a\nabla p)=(\phi/k)(\partial b/\partial t) \quad \ldots\ldots (4)$$

$$\text{and } \nabla\cdot(\alpha\nabla p)=(\phi/k)(\partial\beta/\partial t). \quad \ldots\ldots (5)$$

The nonlinearities of Eqs. 4 and 5, given by coefficients a and α, can be eliminated by introducing an integral transform of the pressure—the pseudopressure function, p_p—defined by Fetkovich.[5] Actually, several pseudopressure functions can be used:

$$p_{po}=\int_{p_0}^{p}\alpha\,dp, \quad \ldots\ldots (6)$$

$$p_{pg}=\int_{p_0}^{p}a\,dp, \quad \ldots\ldots (7)$$

$$\text{and } p_{pt}=\int_{p_0}^{p}(a+\alpha)\,dp. \quad \ldots\ldots (8)$$

Any linear combination of a and α can be used to define p_{pt}—e.g., normalizing Eqs. 4 and 5 before adding. In practical use, the choice of definition depends on reservoir characteristics and test boundary conditions. Eq. 6 is used for an oil reservoir with constant surface oil rate; Eq. 7 is used with constant surface gas rate during the test; and Eq. 8 requires constant total rate of gas plus oil at surface conditions.

To evaluate the integrals in Eqs. 6 through 8, the relationship between S and p must be known. This relationship must be consistent with the pressure and saturation profiles developed around the well during the test. In contrast to the single-phase pseudopressure function, the multiphase pseudopressure functions generally are not uniquely dependent on pressure but depend on the history of the test; e.g., $p_{po}(p)$ for a drawdown test is different from $p_{po}(p)$ for buildup following the drawdown.[6]

Line-Source Solution. For radial flow and with the Boltzmann variable y, $y=\phi r^2/4kt$, Eq. 5 yields

$$(d/dy)[\alpha y(dp/dy)]=-y(d\beta/dy). \quad \ldots\ldots (9)$$

*Now at Norwegian Inst. of Technology.

From Eq. 6 we have $\alpha(dp/dy)=dp_{po}/dy$ and

$$\frac{d\beta}{dy}=\dot{\beta}\frac{dS}{dy}+\beta'\frac{dp}{dy}=\left(\dot{\beta}\frac{dS}{dp}+\beta'\right)\alpha^{-1}\frac{dp_{po}}{dy}.$$

Substituted into Eq. 9, this gives

$$\frac{d}{dy}\left(y\frac{dp_{po}}{dy}\right)=-\left(\frac{c}{\lambda}\right)^{*}y\frac{dp_{po}}{dy}, \quad \ldots\ldots\ldots\ldots\ldots\ldots (10)$$

where $(c/\lambda)^*=[\dot{\beta}(dS/dp)+\beta']\alpha^{-1}$. $\ldots\ldots\ldots\ldots\ldots\ldots (11)$

The term $(c/\lambda)^*$ is a generalized compressibility/mobility ratio. For single-phase flow, it corresponds to the compressibility-viscosity product and for two-phase flow, it corresponds to the total compressibility divided by the total mobility in the approximation given by Martin,[3] as will be verified below.

If $(c/\lambda)^*$ in Eq. 11 is considered constant, then Eq. 10 has the standard line-source solution in the logarithmic approximation,

$$p_{pow}=p_{poi}-\frac{141.2q_o}{kh}\left[\frac{1}{2}\left(\ln\ t_D+0.80907\right)\right], \quad \ldots\ldots\ldots (12)$$

where q_o is the constant surface rate and

$$t_D=0.0002637[kt/\phi r_w^2(c/\lambda)^*]. \quad \ldots\ldots\ldots\ldots\ldots\ldots (13)$$

Field units are used consistently.

Although $(c/\lambda)^*$ can be shown to vary with pressure, our simulation results, as well as those of Raghavan,[6] show that the pseudopressure function plots as a semilog straight line during the entire infinite-acting period. This can be explained from the boundary condition

$$\lim_{y\to 0}\left(y\frac{dp_{po}}{dy}\right)=\frac{141.2q_o}{2kh} \quad \ldots\ldots\ldots\ldots\ldots\ldots (14)$$

used in deriving Eq. 12. That is, when the producing time becomes sufficiently large, Eq. 14 can be solved directly and yields logarithmic time dependence, independent of $(c/\lambda)^*$.

Interpreted results from simulated tests correlate fairly well with the liquid reference curve if the initial value, $(c/\lambda)_i^*$, is used in Eq. 13. To correlate exactly with the liquid reference curve, $(c/\lambda)_i^*$ has to be adjusted by a constant correction factor, usually between 1.0 and 2.0. This is also necessary in Raghavan's[6] example. The slight error in using $(c/\lambda)_i^*$ can be seen as a usually small and negligible amount of skin.

When the well reaches pseudosteady state during a drawdown test, the Boltzmann transform is no longer valid and the boundary condition of Eq. 14 breaks down. In this flow period, the pressure dependence of $(c/\lambda)^*$ can be expected to cause deviations from the liquid reference curve.

Line-source solutions for other choices of pseudopressure functions, defined in Eqs. 7 and 8, can be derived similarly by use of different expressions for $(c/\lambda)^*$.

Relationship Between Saturation and Pressure. From the oil equation (Eq. 9) and the corresponding gas equation, respectively, we get

$$\alpha\frac{d}{dy}\left(y\frac{dp}{dy}\right)+\frac{d\alpha}{dy}y\frac{dp}{dy}=-y\frac{d\beta}{dy} \quad \ldots\ldots\ldots\ldots\ldots (15)$$

and $$a\frac{d}{dy}\left(y\frac{dp}{dy}\right)+\frac{da}{dy}y\frac{dp}{dy}=-y\frac{db}{dy}. \quad \ldots\ldots\ldots\ldots\ldots (16)$$

Here, $da/dy=\dot{a}(dS/dy)+a'(dp/dy)$. The three similar terms can be explicitly expressed in the same way.

For convenience, we introduce $N=y(dp/dy)$ and $K=y(dS/dy)$, so that the respective oil and gas flow equations become

$$\alpha\frac{dN}{dy}+N\cdot\left(\alpha'\frac{N}{y}+\beta'\right)+K\cdot\left(\dot{\alpha}\frac{N}{y}+\dot{\beta}\right)=0$$

and $$a\frac{dN}{dy}+N\cdot\left(a'\frac{N}{y}+b'\right)+K\cdot\left(\dot{a}\frac{N}{y}+\dot{b}\right)=0.$$

Eliminating dN/dy between the two equations and noting that $K/N=dS/dp$, we get the general saturation/pressure relation

$$\frac{dS}{dp}=\frac{(\alpha a'-a\alpha')\dfrac{N}{y}+(\alpha b'-a\beta')}{(a\dot{\alpha}-\alpha\dot{a})\dfrac{N}{y}+(a\dot{\beta}-\alpha\dot{b})}. \quad \ldots\ldots\ldots\ldots\ldots (17)$$

Estimating N/y. From Darcy's law, at radius r and time t,

$$2\pi rkh\alpha(y)[\partial p(y)/\partial r]=q_o(y),$$

where $q_o(y)$ is the surface oil rate. Hence,

$$N=y(dp/dy)=q_o(y)/4\pi kh\alpha(y),$$

which shows that N is bounded for all values of y. At the wellbore,

$$N/y=q_o t/\pi r_w^2 h\alpha\phi \quad \ldots\ldots\ldots\ldots\ldots\ldots\ldots (18a)$$

or $$N/y=(1/\alpha)(t/t_w), \quad \ldots\ldots\ldots\ldots\ldots\ldots\ldots (18b)$$

where $t_w=13.44(\phi r_w^2 h/q_o)$ in field units. Eq. 18 has to be solved iteratively with Eq. 17, because α depends on both saturation and pressure. Note that Eq. 18 is independent of absolute permeability, k. Therefore, p_{po} values can be generated without knowledge of k.

Limiting Cases. We will first examine the two limiting cases of short and long producing times for a constant-surface-oil-rate drawdown test. In these cases, Eq. 17 is solved without estimation of N/y.

Initial Flow: $y\to\infty$ $(t\to 0)$. Because N is bounded, $N/y\to 0$ as $y\to\infty$, and Eq. 17 reverts to

$$dS/dp=(\alpha b'-a\beta')/(a\dot{\beta}-\alpha\dot{b}). \quad \ldots\ldots\ldots\ldots\ldots (19)$$

To compare with Martin's[3] results, we set $r_s=0$, substitute the expressions from Eq. 3, and get

$$\alpha b'-a\beta'=\frac{\lambda_t}{B_oB_g}\left(S_o\frac{B_o'}{B_o}+\frac{\lambda_o}{\lambda_t}c_t\right)$$

and $a\dot{\beta}-\alpha\dot{b}=\lambda_t/B_oB_g$,

where $\lambda_t=\lambda_o+\lambda_g=(k_{ro}/\mu_o)+(k_{rg}/\mu_g)$ and $c_t=-(S_oB_o'/B_o)+(S_oB_gR_s'/B_o)-(S_gB_g'/B_g)$ is the total compressibility of the fluids. Hence,

$$dS_o/dp=S_o(B_o'/B_o)+(\lambda_o/\lambda_t)c_t, \quad \ldots\ldots\ldots\ldots\ldots (20)$$

as shown by Martin.[3]

Eq. 19 can be derived directly from Eqs. 15 and 16 by neglecting the second-order flow terms.[3] Substituting Eq. 20 into Eq. 11, we find $(c/\lambda)^*=c_t/\lambda_t$. Therefore, in the limiting case when $t\to 0$ or if the second-order flow terms can be neglected, the standard interpretation procedure is applicable.[2] Our simulation runs show, however, that Eq. 19 is valid at the wellbore only for very short producing times; i.e., only a few minutes for the presented example.

Long Producing Times: $y\to 0$. In this case, Eq. 17 reduces to

$$dS/dp=(\alpha a'-a\alpha')/(a\dot{\alpha}-\alpha\dot{a}). \quad \ldots\ldots\ldots\ldots\ldots (21)$$

The consequences of this expression can be seen as follows. The producing GOR is given by $R=a/\alpha$. The total derivative of R with respect to pressure is then $dR/dp=\dot{R}(dS/dp)+R'$. Substituting from Eq. 21, we find that $dR/dp=0$; i.e., the GOR is a constant, independent of pressure and time. This is an important observation. For

a drawdown test in the infinite-acting period, when Eq. 21 becomes valid, the GOR will stabilize. The stabilization level depends strongly on the rate and may be higher or lower than the initial GOR, as observed from our simulation runs. The stabilization and the shift from Eq. 19 to 21 occur after a very short producing time. Eq. 21 easily can be derived from Eqs. 15 and 16 by neglecting the expansion terms on the right side of the equations.

Saturation as a Function of Radius. In the infinite-acting period when the Boltzmann transform is valid, saturation and pressure profiles can easily be generated if S and p are known functions of time at the wellbore.

For a drawdown test, at r_1 and t_1, S will be equal to the saturation at the wellbore at $t_2=(r_w^2/r_1^2)t_1$.

During buildup, the saturation change, ΔS, from the shut-in profile, at r_1 and shut-in time, Δt_1, will be equal to the saturation change at the wellbore at shut-in time, Δt_2, given by $\Delta t_2=(r_w^2/r_1^2)\Delta t_1$.

Integration Paths. Raghavan[6] pointed out that the pseudopressure function should reflect the pressure and saturation profiles occurring in the drainage area during the test. To achieve this, the integral $\int_{p_w}^{p_i}\alpha dp$ could, for a given time, be evaluated by integration over the saturation and pressure profiles—i.e., along r. This approach is consistent with the pseudopressure equations suggested for steady-state and pseudosteady-state (PSS) flow by Fetkovich.[5] When the Boltzmann transform is valid, however, the integration along the radius for a fixed time is equivalent to the integration over time for a fixed radius, $r=r_w$. Therefore, in the infinite-acting period, the pseudopressure function can be evaluated simply by using the correct pressure/saturation relation at the wellbore.

Interpretation Procedures, Infinite-Acting Period. ***Drawdown.*** Eqs. 17 and 18 are used to generate S vs. p_{wf} in tabular form. The pseudopressure function, p_{po}, is calculated from Eq. 6. A semilog plot of p_{po} vs. producing time, t, gives a straight line and absolute permeability, k, is calculated from the slope. The dimensionless pseudopressure function, p_{pwD}, can then be calculated and compared with the liquid-reference curve,

$$p_{pwD}=(kh/141.2q_o)p_{pw}, \quad \ldots\ldots\ldots\ldots\ldots\ldots\ldots\ldots\ldots\ldots (22)$$

TABLE 1—RESERVOIR PROPERTIES

ϕ	0.30
k, md	10.0
p_i, psia	5,704.0
p_{bi}, psia	5,704.0
s_{iw}, incompressible	0.30
s_{gi}	0.0
r_w, ft	0.33
r_e, ft	656.0
h	15.6

where $p_{pw}=p_{po}(p_i)-p_{po}(p_{wf})=\int_{p_{wf}}^{p_i}\alpha dp$.

This method is similar to that suggested by Raghavan,[6] who used the GOR equation, $R=a/\alpha$, to relate saturation to pressure on the basis of measured values of R.

Buildup. The saturation/pressure relation at the wellbore during buildup differs from the drawdown case. After shut-in, the pressure gradient at the wellbore is zero and $N/y=0$. Hence, Eq. 19 is valid during the entire buildup period. The saturation at the wellbore at the instant of shut-in can be found from drawdown S vs. p, or directly from the GOR equation and the observed constant level of R. S vs. p_{ws} is generated in tabular form with Eq. 19, and p_{pwD} is obtained from

$$p_{pwD}=(kh/141.2q_o)p_{pw}, \quad \ldots\ldots\ldots\ldots\ldots\ldots\ldots\ldots\ldots\ldots (23)$$

where $p_{pw}=p_{po}(p_{ws})-p_{po}(p_{wf,s})=\int_{p_{wf,s}}^{p_{ws}}\alpha dp$.

If the saturation/pressure relation at the wellbore had been valid for all radii, a Horner plot of p_{pwD} from Eq. 23 would have yielded the formation permeability. The numerical examples below demonstrate that this is not the case.

Raghavan[6] suggested a different procedure for calculating p_{pw} for buildup test interpretation. The S vs. p relation is derived from the GOR equation with R held constant at the shut-in value.

PSS. ***Drawdown.*** When the well reaches PSS, the Boltzmann transform is no longer compatible with boundary conditions. If the use of Eq. 17 is extended into this flow period, deviation from the liquid analogy will occur. Even if the correct S-vs.-p relation at the wellbore were used, from the observed $R=a/\alpha$, it is not obvious that a continued integration of only wellbore data would give a pseudopressure function that properly describes the conditions within the drainage area. Also, $(c/\lambda)^*$ in the expression for dimensionless time (Eq. 13) varies with pressure and may cause deviation from the liquid reference curve. Therefore, it is not evident whether the liquid analogy of multiphase flow can be extended into the PSS period to determine the drainage area accurately.

Buildup From PSS. It can easily be shown, without the Boltzmann transform, that the S-vs.-p relation at the wellbore still is given by Eq. 19. This is verified in the presented example. But, if the pseudopressure function is evaluated on the basis of wellbore data only, the corresponding Horner plot will not be a straight line with the correct slope, as shown in the example. This also indicates that for buildup from PSS, a pseudopressure function evaluated from the correct wellbore data will not properly describe the saturation and pressure profiles occurring in the reservoir during the test. It appears that Raghavan's[6] suggested procedure for buildup better covers this case. The lack of a liquid analogy makes it difficult to determine the average reservoir pressure accurately from the test.

TABLE 2—FLUID PROPERTIES*

p (psia)	B_o (res m³/stock-tank m³)	μ_o (cp)	R_s (std m³/stock-tank m³)	$1/B_g$ (std m³/res m³)	μ_g (cp)
5,705	1.806	0.298	266.964	298.85	0.0298
5,633	1.791	0.300	261.867	296.99	0.0295
5,204	1.702	0.317	232.513	285.12	0.0281
4,703	1.605	0.348	200.793	269.48	0.0263
4,202	1.516	0.391	171.590	251.30	0.0246
3,700	1.434	0.446	144.715	229.88	0.0228
3,200	1.360	0.515	119.997	204.59	0.0210
2,770	1.302	0.587	100.408	179.63	0.0195
2,340	1.249	0.671	82.196	151.96	0.0181
1,911	1.202	0.768	65.275	122.42	0.0166
1,482	1.159	0.881	49.553	92.32	0.0152
1,052	1.121	1.011	34.925	63.03	0.0138
623	1.088	1.164	21.218	35.63	0.0125
193	1.058	1.35	7.887	10.55	0.0113

*PVT properties represent a crude oil system with 35°API oil, specific gas gravity of 0.75, initial solution GOR of 1,500 scf/STB, and reservoir temperature of 200°F.

TABLE 3—RELATIVE PERMEABILITIES

Relative permeabilities are generated as table input to the model from the following expressions.

$$k_{ro} = 0.7(S_o^*)^4$$
$$k_{rg} = 0.7(1 - S_o^*)^2[1 - (S_o^*)^2]$$
$$S_o^* = S_o/(1 - S_{iw})$$
$$S_{iw} = 0.30$$

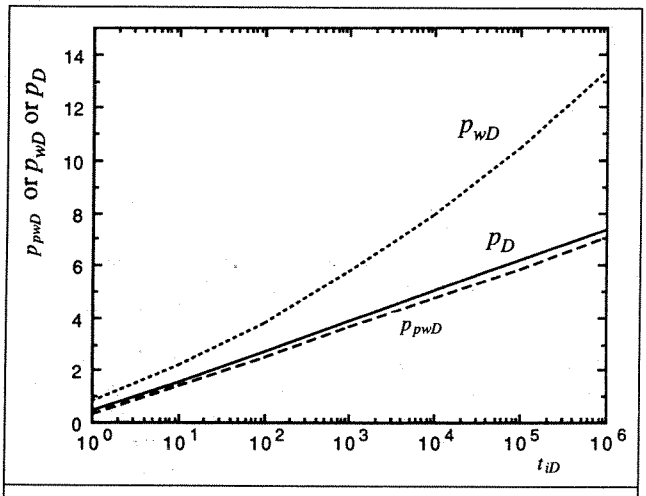

Fig. 1—Dimensionless pressure functions vs. dimensionless producing time, t_{iD}: Case 1 with $q_o = 125.8$ STB/D.

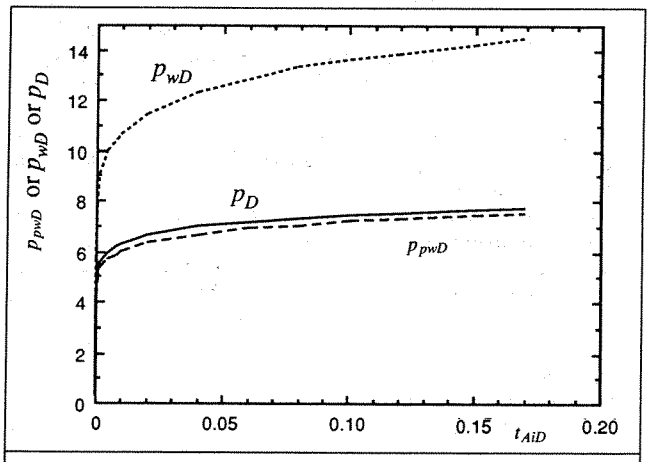

Fig. 2—Dimensionless pressure functions vs. dimensionless time, t_{AiD}: Case 1 with $q_o = 125.8$ STB/D.

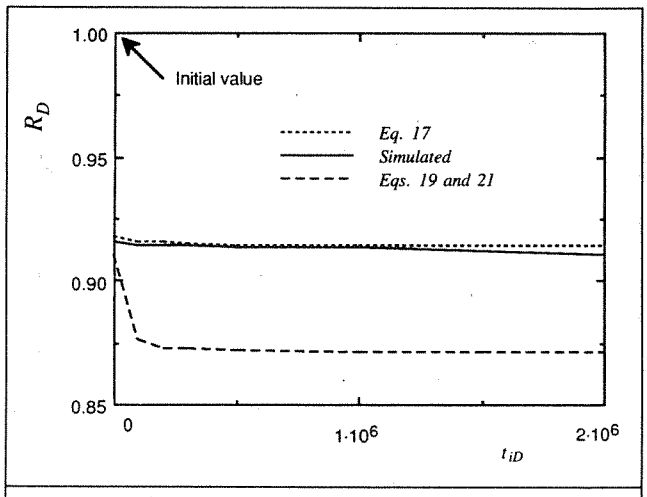

Fig. 3—Dimensionless producing GOR, R_D, vs. dimensionless time, t_{iD}: Case 1 with $q_o = 125.8$ STB/D.

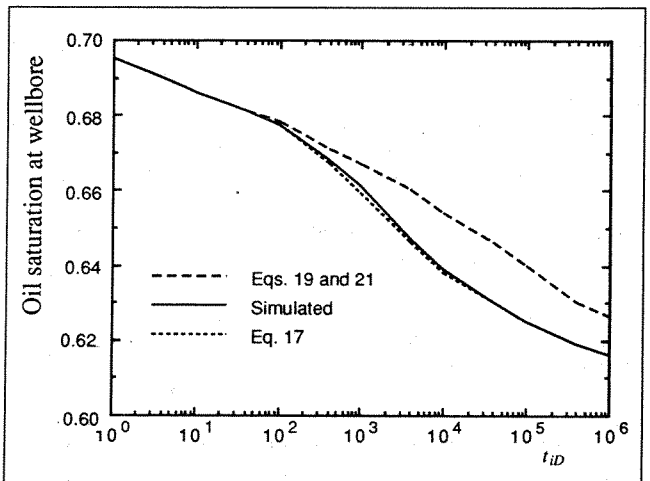

Fig. 4—Oil saturation at wellbore vs. dimensionless time, t_{iD}: Case 1 with $q_o = 125.8$ STB/D.

Example

Numerical Model. The test data were generated by a radial, 1D, three-phase simulator with variable bubblepoint pressure. The formulation is implicit finite difference with simultaneous and direct solution of pressures and saturations.

The validity of the model was checked by simulation and interpretation of several single-phase-liquid pressure tests. Trial runs were made to eliminate time and space discretization errors. All example runs were made with a 40-block numerical grid, the block lengths increasing logarithmically with radius, and with the timestep size controlled by a maximum saturation change of 0.025 and maximum pressure change of 43.5 psi [300 kPa].

Reservoir and Test Characteristics. Example tests are limited to a well fully penetrating the center of a radial oil reservoir with solution-gas drive. Therefore, in all calculations, the oil pseudopressure function from Eq. 6 is used. The base case was made with a constant surface-oil rate of 125.8 STB/D [20 stock-tank m^3/d]. All runs had incompressible water at an irreducible saturation of 0.30 and started with initial reservoir pressure equal to the bubblepoint pressure. The absolute permeability and porosity were constant, and gravitational and capillary effects were excluded. The common reservoir properties, fluid properties, and relative permeabilities for the tests are presented in Tables 1, 2, and 3, respectively.

Dimensionless Variables. All plots are presented in dimensionless form with the pseudopressure functions, p_{pwD}, for drawdown and buildup defined by Eqs. 22 and 23. Dimensionless time, t_{iD}, based on wellbore radius is defined by Eq. 13, with $(c/\lambda)^*$ evaluated at initial pressure. Dimensionless time based on drainage area, t_{AiD}, is given by

$$t_{AiD} = t_{iD}(r_w^2/\pi r_e^2).$$

Dimensionless wellbore pressures, p_{wD}, for drawdown and buildup, respectively, are defined by

$$p_{wD} = (kh/141.2q_o)(p_i - p_{wf})$$

and $p_{wD} = (kh/141.2q_o)(p_{ws} - p_{wf,s})$.

Note that k_{roi} is not included in the definition of p_{wD}. Correct slope of a p_{wD}-vs.-t_{iD} semilog plot should therefore be $1.151/k_{roi}$ per log cycle, while for the corresponding p_{pwD} plots, the slope should be 1.151 per log cycle.

The dimensionless liquid reference pressure is denoted by p_D on the plots.

Test Cases. The following tests were simulated and analyzed.

Case 1. Drawdown to 100 hours corresponds to $t_{AiD} = 0.17$. The test extends slightly into PSS ($t_{AiD} > 0.10$), for rates $q_o = 62.9$,

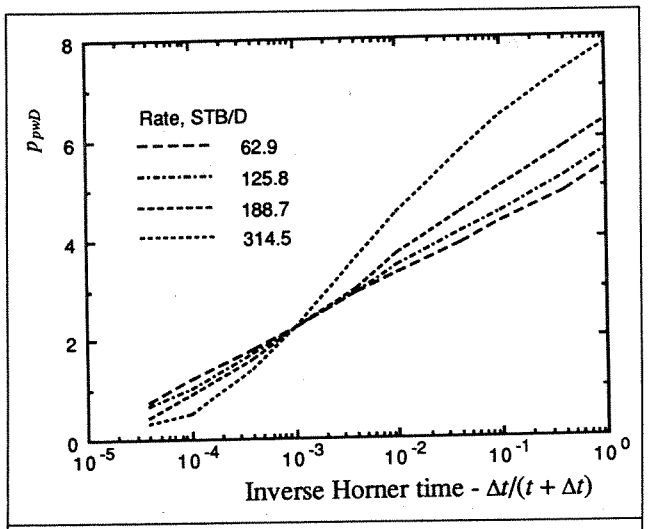

Fig. 5—Dimensionless pseudopressure function, p_{pwD}, vs. inverse Horner time for several rates: Case 2.

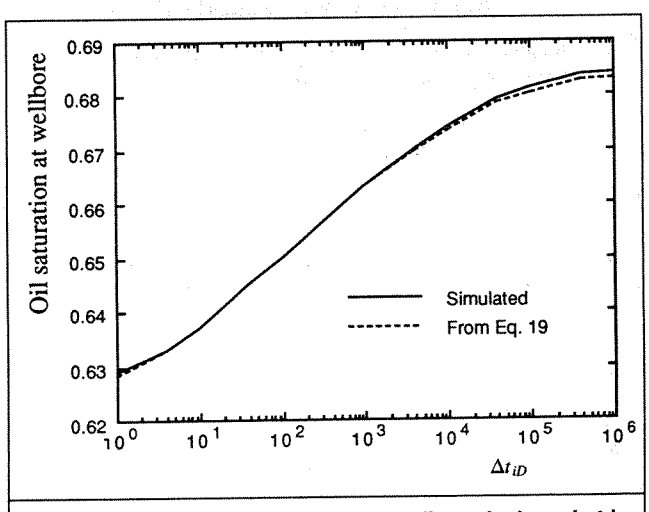

Fig. 6—Oil saturation at the wellbore vs. dimensionless shut-in time, Δt_{ID}: Case 2 with q_o = 125.8 STB/D.

125.8, 188.7, and 251.6 STB/D [10, 20, 30, and 40 stock-tank m³/d]. Drawdown to t_{AiD}=2.7 with q_o=125.8 STB/D [20 stock-tank m³/d].

Case 2. Buildup follows a drawdown of 5 hours. The entire tests were performed in the infinite-acting period with rates q_o=62.9, 125.8, 188.7, and 314.5 STB/D [10, 20, 30, and 50 stock-tank m³/d].

Case 3. Buildup begins at PSS with q_o=125.8 STB/D [20 stock-tank m³/d] and with producing time t=100 and 2,500 hours.

Results. ***Case 1.*** A semilog plot of pseudopressure function, p_{pwD}, liquid reference pressure, p_D, and wellbore pressure, p_{wD}, is shown in Fig. 1 for q_o=125.8 STB/D [20 stock-tank m³/d] because the other rates gave almost identical results for p_{pwD}. As shown, this curve is a straight line, with the correct slope in the infinite-acting period, parallel to the liquid reference curve. A slight shift between the two curves corresponds to a correction factor of 1.62 on $(c/\lambda)_i^*$, or a skin factor equal to −0.48, which should have been zero because no fixed skin zone is used in the model and gas blockage around the well is incorporated in the p_{pwD} function. The p_{pwD} plot, therefore, will give the correct absolute permeability, but a slightly erroneous skin factor if $(c/\lambda)_i^*$ is used in the dimensionless time, t_{iD}. The p_{wD} values do not plot as a straight line and cannot be used to interpret the test.

The results are replotted in Fig. 2 on a linear t_{AiD} scale. The infinite-acting S-vs.-p relation from Eq. 17 also has been used to evaluate p_{pwD} in the PSS period. The slope of the p_{pwD} curve is close to the correct value, 2π, but the shift between the p_D and p_{pwD} curves makes drainage-area determination uncertain. Further extension of the drawdown to t_{AiD}=2.7 shows that the p_{pwD} values do not plot as a straight line, as also noted by Raghavan.[6] Neither of the two suggested methods, therefore, is applicable for a liquid-analogy interpretation in the PSS period.

Fig. 3 shows the development of producing GOR with time for q_o=125.8 STB/D [20 stock-tank m³/d]. The simulated and calculated R values from Eq. 17 agree closely. $R_D=R/R_{si}$ drops down from 1.0 within about 5 minutes and then stays constant throughout the infinite-acting period. The third curve was generated with Eq. 19 until dS/dp became equal to the value calculated from Eq. 21, and then Eq. 21 was applied. Only a coarse estimate of the constant R level is achieved.

Fig. 4 plots simulated and calculated values of the oil saturation at the wellbore. There is a close agreement between simulated values and values from Eq. 17.

Case 2. Fig. 5 depicts the results from buildup following the 5-hour drawdown in a Horner plot for the rates q_o=62.9, 125.8, 188.7, and 314.5 STB/D [10, 20, 30, and 50 stock-tank m³/d], demonstrating a significant rate dependence. Therefore, even though Eq. 19 precisely monitors the saturation at the wellbore, as shown in Fig. 6, it will not transform the wellbore pressures into a correct, liquid-analogy pseudopressure function.

Simulated and calculated saturation profiles as functions of radius, at shut-in and after a 5-minute buildup, are given in Fig. 7. The calculated saturations were generated from wellbore data by the

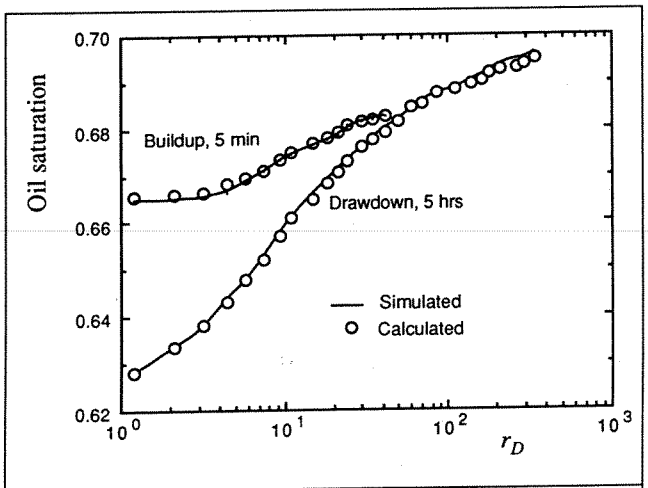

Fig. 7—Saturation profiles vs. dimensionless radius, r_D, at the end of 5-hour drawdown and after 5-minute buildup: Case 2 with q_o = 125.8 STB/D.

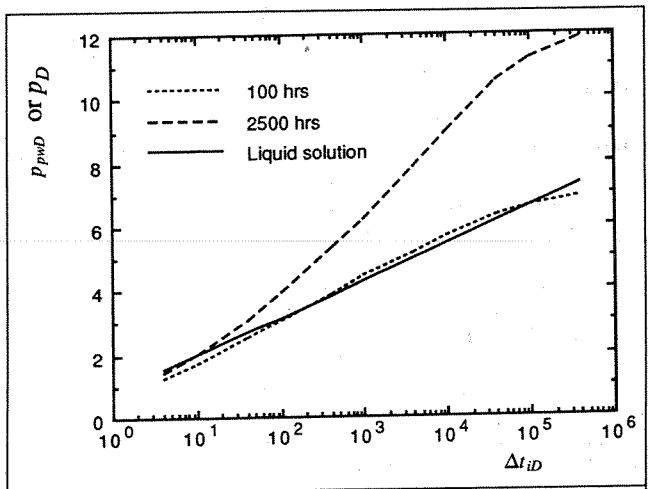

Fig. 8—Dimensionless pressure functions vs. dimensionless shut-in time, Δt_{ID}, following producing times of 100 and 2,500 hours: Case 3 with q_o = 125.8 STB/D.

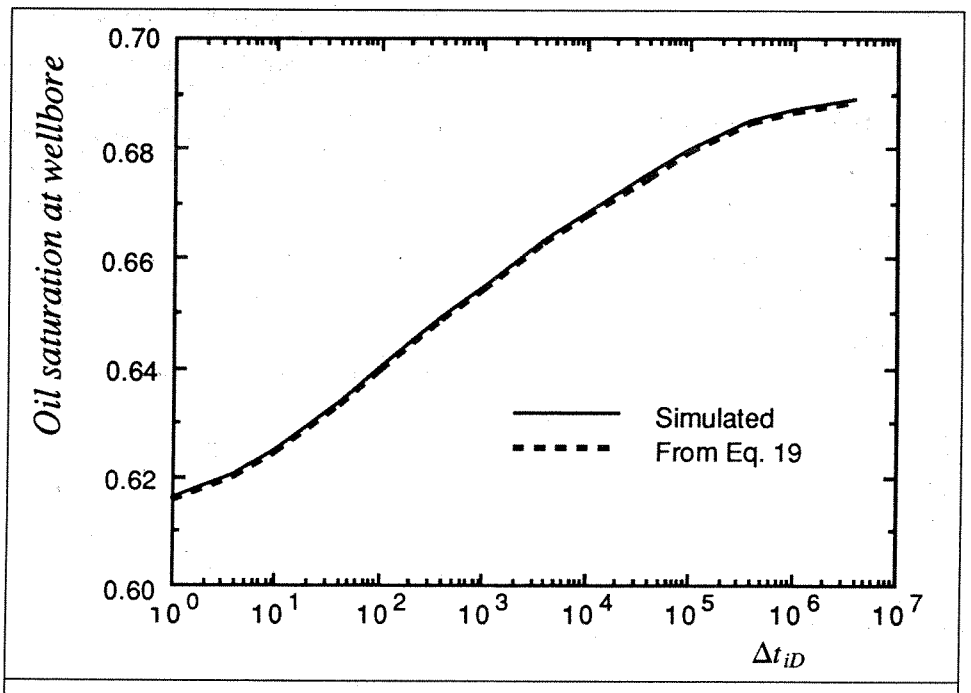

Fig. 9—Oil saturation at the wellbore vs. dimensionless shut-in time, Δt_{iD}: Case 3 with $q_o = 125.8$ STB/D.

Boltzmann transform variable. The excellent agreement for the drawdown case demonstrates the validity of the transform in the infinite-acting period. For this rate, $q_o = 125.8$ STB/D [20 stock-tank m^3/d], there is also a good match for buildup following drawdown.

Case 3. Fig. 8 gives modified Horner plots for buildups following 100 and 2,500 hours of drawdown with a rate of 125.8 STB/D [20 stock-tank m^3/d], together with the liquid reference curve. Eq. 19 was used to generate the pressure/saturation relation, and, as shown in Fig. 9, the relation is correct at the wellbore. Although the correct relationship between pressure and saturation at the wellbore is used, the p_{pwD} function generated from these data departs from the liquid analogy. This is probably because wellbore data alone will not properly represent the saturation and pressure profiles that occur in the reservoir during buildup from PSS.

Conclusions

1. Theoretical developments are strictly valid when there is a unique relation between pressure and saturation. This is the case for a drawdown test in the infinite-acting period.
2. For buildup, a correct pressure/saturation relation at the wellbore is given. The associated pseudopressure function, however, cannot be used to interpret the test.
3. During a drawdown test, the producing GOR quickly stabilizes and remains constant throughout the infinite-acting period.

Nomenclature

a = parameter defined by Eq. 3b, scf/RB-cp [std m^3/res m^3·Pa·s]
b = parameter defined by Eq. 3d, scf/RB [std m^3/res m^3]
B_g = gas FVF, RB/scf [res m^3/std m^3]
B_o = oil FVF, RB/STB [res m^3/stock-tank m^3]
c = compressibility, psi^{-1} [kPa^{-1}]
$(c/\lambda)^*$ = $[\beta(dS/dp)+\beta']\alpha^{-1}$, generalized compressibility/mobility ratio, cp/psi [Pa·s/kPa]
h = formation height, ft [m]
k = absolute permeability, md
k_r = relative permeability, dimensionless
K = $y(dS/dy)$, dimensionless
N = $y(dp/dy)$, psi [kPa]
p = pressure, psi [kPa]
p_b = bubblepoint pressure, psi [kPa]
p_p = pseudopressure function defined by Fetkovich[5]*
p_{po} = oil pseudopressure function, STB-psi/RB-cp [stock-tank m^3·kPa/res m^3·Pa·s]
p_{wf} = flowing well pressure, psi [kPa]
$p_{wf,s}$ = flowing well pressure at shut-in, psi [kPa]
p_{ws} = shut-in well pressure, psi [kPa]
p_0 = base pressure in evaluation of pseudopressure function, psi [kPa]
q_o = oil surface flow rate, STB/D [stock-tank m^3/d]
r = radius, ft [m]
r_D = r/r_w, dimensionless radius
r_s = dissolved oil/gas ratio, STB/scf [stock-tank m^3/std m^3]
R = producing GOR, scf/STB [std m^3/stock-tank m^3]
R_D = R/R_{si}, dimensionless producing GOR
R_s = solution GOR, scf/STB [std m^3/stock-tank m^3]
S = saturation or oil saturation
S_{iw} = irreducible water saturation
S_o^* = $S_o/(1-S_{iw})$, normalized oil saturation, dimensionless
ΔS = saturation change during buildup, at a fixed radius
t = time or producing time, hours
Δt = shut-in time, hours
x = dummy variable
y = $\phi r^2/4kt$, Boltzmann variable, ft^2/md-hr [m^2/μm^2·hr]
α = parameter defined by Eq. 3c, STB/RB-cp [stock-tank m^3/res m^3·Pa·s]
β = parameter defined by Eq. 3e, STB/RB [stock-tank m^3/res m^3]
λ = k_r/μ, mobility, cp^{-1} [(Pa·s)$^{-1}$]
μ = viscosity, cp [Pa·s]
ϕ = porosity

Subscripts

AiD = dimensionless, based on drainage area and with $(c/\lambda)^*$ evaluated at p_i

*Fetkovich uses the symbol "m."

D = dimensionless
e = external
g = gas
i = initial
iD = dimensionless, with $(c/\lambda)^*$ evaluated at p_i
o = oil
t = total
w = well or water
1 = denotes a chosen, arbitrary point (r_1,t_1) for drawdown or $(r_1,\Delta t_1)$ for buildup
2 = denotes time t_2 when $S(r_w,t_2)=S(r_1,t_1)$ for drawdown, or time Δt_2 when $\Delta S(r_w,\Delta t_2)=\Delta S(r_1,\Delta t_1)$ for buildup

Superscripts

$\cdot$ = operator, partial derivative with respect to S at constant p
$'$ = operator, partial derivative with respect to p at constant S

Acknowledgments

We appreciate the economic support from the Royal Norwegian Council for Industrial and Scientific Research (Grant No. 1840.07425) and from Statoil.

References

1. Al-Hussainy, R., Ramey, H.J. Jr., and Crawford, P.B.: "The Flow of Real Gases Through Porous Media," *JPT* (May 1966) 624–36; *Trans.*, AIME, **237**.
2. Perrine, R.L.: "Analysis of Pressure Buildup Curves," *Drill. & Prod. Prac.*, API, Dallas (1956) 482.
3. Martin, J.C.: "Simplified Equations of Flow in Gas Drive Reservoirs and the Theoretical Foundations of Multiphase Pressure Buildup Analyses," *Trans.*, AIME (1959) **216**, 309–11.
4. Weller, W.T.: "Reservoir Performance During Two-Phase Flow," *JPT* (Feb. 1966) 240–46; *Trans.*, AIME, **237**.
5. Fetkovich, M.J.: "The Isochronal Testing of Oil Wells," paper SPE 4529 presented at the 1973 SPE Annual Meeting, Las Vegas, Sept. 30–Oct. 3.
6. Raghavan, R.: "Well Test Analysis: Wells Producing by Solution Gas Drive," *SPEJ* (Aug. 1976) 196–208; *Trans.*, AIME, **261**.
7. Whitson, C.H. and Torp, S.B.: "Evaluating Constant-Volume Depletion Data," *JPT* (March 1983) 610–20.

SI Metric Conversion Factors

°API	141.5/(131.5+°API)		=	g/cm^3
bbl	× 1.589 873	E−01	=	m^3
cp	× 1.0*	E−03	=	Pa·s
ft	× 3.048*	E−01	=	m
°F	(°F−32)/1.8		=	°C
md	× 0.986 923	E−04	=	μm^2
psi	× 6.894 757	E+00	=	kPa
psi^{-1}	× 1.450 377	E−01	=	kPa^{-1}
scf/bbl	× 1.801 175	E−01	=	m^3/m^3

*Conversion factor is exact.

SPEFE

Original SPE manuscript received for review Nov. 5, 1982. Paper accepted for publication April 19, 1989. Revised manuscript received April 10, 1989. Paper (SPE 10224) first presented at the 1981 SPE Annual Technical Conference and Exhibition held in San Antonio, Oct. 5–7.